Study of interfacial microstructure in hybrid additive manufactured aluminium alloys

Mpinda Bob Mampuya[1*], *Ngeleshi Mike* Kibambe[1], *Mutombo Christian* Umba[1], *Olusoji Oluremi* Ayodele[1], and *Peter Apata* Olubambi[1]

[1] Centre for Nanoengineering and Advanced Materials, School of Mining, Metallurgy and Chemical Engineering, University of Johannesburg, South Africa

Abstract. Traditional manufacturing procedures have been used to make aluminium alloy engineering components for decades, but machining stages add cost and lead time. Today, the aerospace and automotive sectors use Selective Laser Melting (SLM) technologies to make near-net-shaping parts with complex geometry. This method of melting powder alloys layer-by-layer using a high-energy laser is limited to small component sizes, while traditional manufacturing processes can handle large components. A hybrid additive manufacturing (HAM)-subtractive manufacturing (SM) technology has been developed for creating complex geometry and large aluminium alloy components. The laser interacts with the powder bed on a substrate to form a molten pool that solidifies quickly when cooled during SLM. The interfacial phenomena can be directly affected by heat transfer, element dilution, diffusion, solidification dynamics, and phase transformations, which are responsible for the significant changes in the alloy's microstructure. Optical Microscope (OM), Scanning Electron Microscopy (SEM) coupled with Electron Dispersive X-Ray Spectroscopy (EDX), X-Ray Diffraction (XRD), and microhardness were used to assess the microstructure evolution at the interface bonded zone of a cold-rolled AA 5083 and a 3D-printed $AlSi_{10}Mg$.

1 Introduction

Additive manufacturing (AM) of metallic alloys has transformed modern production by providing exceptional design flexibility, expedited prototyping, and facilitating the creation of both simple and complex innovative engineering parts. Despite the capability of powder-bed technologies such as SLM to produce components with high geometric complexity and optimised material usage or structural performance, their modest build-up rates and limited print volumes constrain component dimensions and the viability of several applications. The synergies between SLM as an AM technique and forging/casting as a traditional manufacturing technique present a distinct opportunity to reconcile complex, bespoke components with production efficiency, guaranteeing that the future of metal additive

* Corresponding author: bobmampuya@gmail.com

manufacturing not only facilitates limitless design innovation but also expedites manufacturing processes, meeting the increasing demand for economical, high-quality parts across various industries.

One of the main outcomes of this research has been the creation of innovative methods to increase the applicability of AM procedures for high-strength aluminium alloys, such as HAM technologies. For particular purposes and needs, HAM combines an AM process with one or more additional processes (typically other AM operations and/or conventional manufacturing) to produce a better end product than could be produced by AM alone or by conventional manufacturing [1,2]. Over the past years, processes, equipment and multi-materials have been integrated and mixed with one another in HAM techniques to improve part quality, performance and mechanical properties [3,4].

Nonetheless, research on the interface analysis of hybrid-built reactive materials, such as those made of aluminium alloys, is very scarce. Chan et al.(2021) [4] investigated the interfacial microstructure and mechanical integrity in a hybrid additive manufacturing process involving a 3D-printable aluminium alloy deposited onto dissimilar wrought aluminium substrates. The authors' study combined microstructural analysis and mechanical testing to evaluate bonding quality at the interface. Results revealed that despite compositional differences, metallurgical bonding was achieved, with fracture consistently occurring in the weaker heat-affected zone (HAZ) rather than along the interface, which indicates effective fusion between the deposited and substrate materials. This work highlights the potential of HAM to achieve structurally sound joints between dissimilar aluminium alloys, thereby informing current efforts to improve interface performance in multi-material builds. Silva et al.(2022) [5] investigated a hybrid manufacturing approach combining additive and subtractive processes using powder and wrought aluminium alloys of similar composition. Their study aimed to assess the sustainability and performance of the resulting components, with particular emphasis on the effects of stress-relief heat treatment on physical, mechanical, and thermal properties. Hadadzadeh et al.(2020) [6] discussed the microstructure and mechanical behaviour of dissimilar materials SLMed $AlSi_{10}Mg$ on an Al-Cu-Ni-Fe-Mg cast alloy substrate. The study found that the bonding between the AlSi10Mg and the cast alloy substrate was strong, indicating good interfacial bonding. The authors suggested that SLM is a viable method for fabricating two-material components with improved mechanical properties.

Building on this emerging body of work, the aim of the present study is to investigate the interfacial microstructure and bonding characteristics in HAM of aluminium alloys, specifically focusing on the joining bond between 3D-printed $AlSi_{10}Mg$ and cold-rolled AA 5083 substrate. While prior studies have demonstrated the feasibility of hybrid builds and highlighted the importance of interfacial integrity, few have conducted detailed microstructural and phase analysis of the interface between dissimilar aluminium alloys within a HAM context. This research addresses that gap by employing a detailed microstructural characterisation and phase transformation. The outcomes of this study contribute to a deeper understanding of interface behaviour in aluminium-based HAM systems and support the broader goal of advancing hybrid manufacturing approaches for lightweight, high-performance structural components.

2 Materials and methods

2.1 Materials

The selected powder material for the AM technique was the gas atomised $AlSi_{10}Mg$ supplied by SLM Solutions Group AG, Germany, with particle sizes of 66.43 µm, 46.45 µm and 27.97 µm, respectively, passing 90%, 50% and 10%. The laser diffraction-based particle size analyser Microtrac S3500 was used to measure the size distribution of particles (Fig. 1c). The SEM image of $AlSi_{10}Mg$ powder (Fig. 1a) indicates that grain morphology is nearly spherical, and the presence of satellites and splats is noticed. Hulamin (Pty) Ltd, Pietermaritzburg, South Africa, supplied the conventional cold-rolled Al alloy AA 5083 sheet that was selected as the base substrate, due to its excellent mechanical properties and exceptional weldability. The chemical compositions of the 3D printed $AlSi_{10}Mg$ and substrate, analysed through Q4 Tasman: Bruker Spark Optical Emission Spectrometer (OES), are listed in Table 1.

Table 1. Chemical composition of materials

	Al	Si	Mg	Fe	Mn	Ti	Zn	Cu	Pb	Sn	Cr
$AlSi_{10}Mg$	Bal	9.90	0.28	0.37	0.01	0.08	0.26	0.14	0.007	0.006	0.024
AA 5083	Bal	1.64	6.88	0.17	0.35	0.014	0.027	0.032	0.006	0.005	0.111

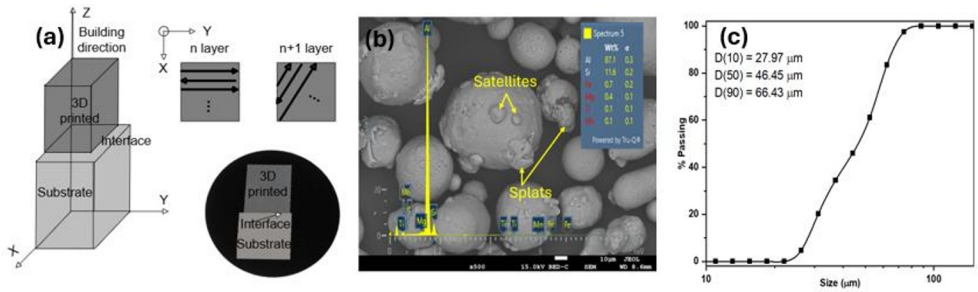

Fig. 1. (a) Schematic diagram of HAM showing the building direction, scanning strategy and the image on the MultiFast mounted. (b) SEM-EDX of the $AlSi_{10}Mg$ powder. (c) Particle size distribution of the $AlSi_{10}Mg$ powder.

2.2 HAM processing

The as-received cold-rolled Al alloy AA 5083 substrate at room temperature was cleaned with acetone to remove any impurities. On the cleaned surface, a progressive build-up deposition of AlSi10Mg powder was made through a selective laser melting process using an SLM®280 (Nikon SLM Solutions) with a continuous wave ytterbium-doped fibre laser. The $AlSi_{10}Mg$ powders were printed in an argon environment to decrease the oxygen concentration to below 0.1%. The commercial recommended printing parameters were applied:

- Laser power: 370 W
- Hatch spacing: 100 µm
- Scan speed: 1650 mm/s
- Layer thickness: 60 µm
- Scan pattern: Stripes, 10 mm wide, 67° rotation angle

2.3 Sample preparation and characterisation

This study focuses on the metallurgical behaviour of hybrid-built components, particularly at the fusion bonded interface. The representative sample was sectioned in a way that both the as-built, the interface and the substrate are hot-mounted in the same MultiFast conductive phenolic resin (Fig. 1a). Metallographic studies were carried out using an OM Olympus GX51 and a SEM JOEL 7900 coupled with EDX on a previously mechanically ground sample with silicon carbide sandpapers, then polished with diamond suspension, followed by a mirror polish with colloidal silica suspension. To reveal the microstructure, Keller's chemical etchant (2ml HF, 3ml HCl, 5ml HNO_3 and 190ml H_2O) was used. Innovatest Falcon 500 microhardness tester was used to perform 10 indentations on each zone. The applied load was set at 50 gf with a dwell time of 10 sec. The XRD presented for phase identification at different zones was conducted with a Rigaku Ultima IV. The scanning range was from 20 to 90° with a 0.01° step width. The processed data used the PDXL 2 software.

3 Results and discussion

3.1 Microstructure analysis

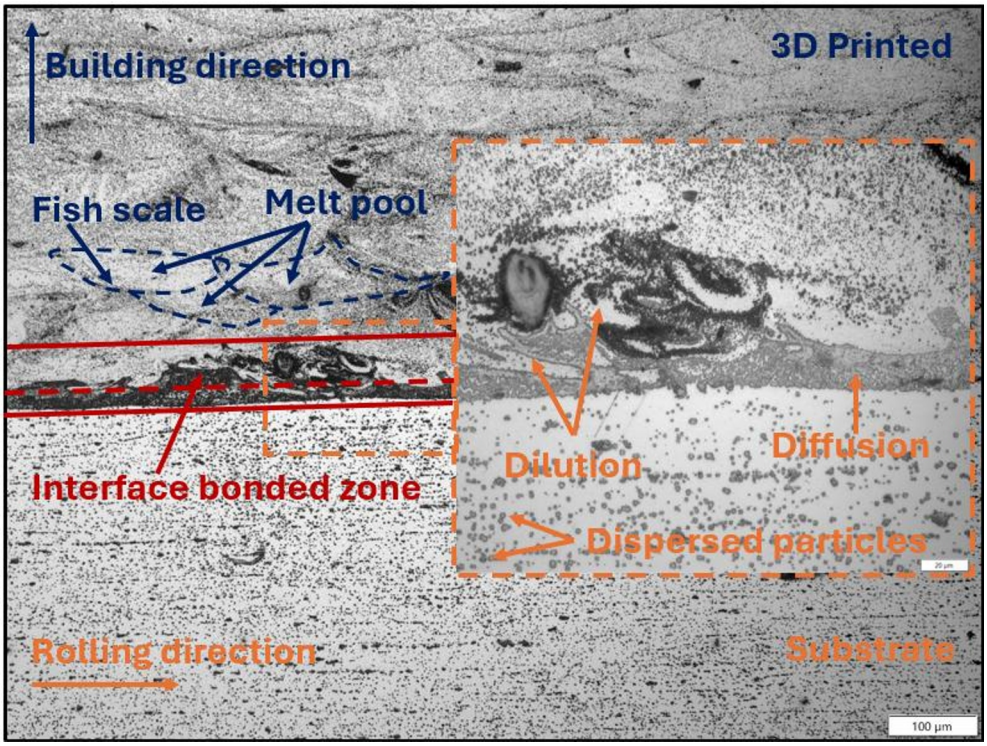

Fig. 2. Optical micrograph of the HAM showing the interface bonded zone between the as-built and the substrate

The microstructural examination of the HAM specimen revealed the presence of 3 distinct zones under low and high magnification. The as-built $AlSi_{10}Mg$ occupies the upper half, substrate material is positioned in the lower half, with the interface bonded zone situated in between (Fig. 1a). The thickness of the interface was defined as the distance over which

the transfer of the two primary alloy elements, Si and Mg, occurred and was located at the zone where the microstructure changed between the 3D printed and substrate material.
The microstructure of the as-built $AlSi_{10}Mg$ comprised ultrafine columnar dendrites oriented along the building direction, as the highest thermal gradient aligns with this direction during the SLM process [7]. The dendritic microstructure of the as-built $AlSi_{10}Mg$ consists of cellular primary α-Al encased by a continuous network of Si-rich eutectic boundaries. The grain morphology exhibited a bimodal structure comprising equiaxed and columnar grains, with columnar grains predominating in the melt pool regions. The equiaxed grains predominantly exhibited the melt pool walls, in which a partial melting of the formerly deposited layer transpired during the melting of the subsequent powder layer [8].

The substrate microstructure exhibited a mixture of fine equiaxed grains and coarse elongated grains in the rolling direction. A combination of solid solution and dispersed particles can be clearly seen. The cold-rolled substrate microstructure generally comprises α-Al dendrites, in which the alloy's principal constituent, Al, crystallises. Intermetallic precipitates, such as $Al_6(Fe,Mn)$ and Mg_2Si, are also present in interdendritic zones.

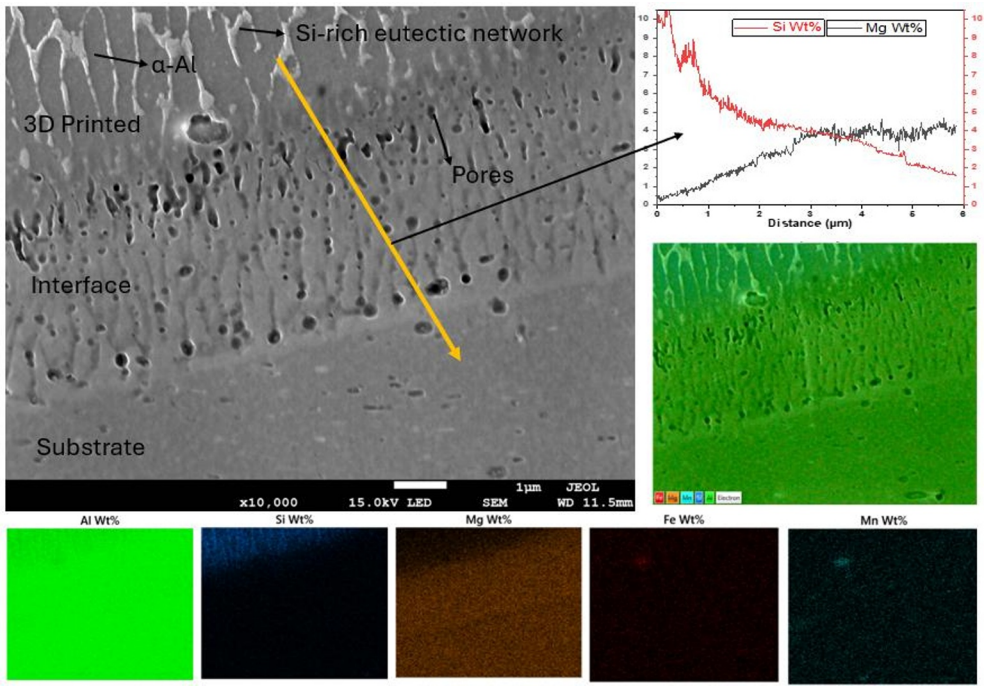

Fig.3. SEM micrograph with element mapping and line scan across the interface bonded zone.

Fig.2. presents a low magnification optical micrograph of the interface bonded zone in the hybrid component, dilution and diffusion of constituent elements are observed, and their metallurgical mechanism is explained by the Marangoni convection observed in the interfacial melt pool. Circular flows induced by the Marangoni effect are observed, which may be enhanced by the underlying Al substrate. The thermal Marangoni convection is directly proportional to surface tension and temperature gradient [9]. The elevated thermal conductivity of the Al substrate amplifies the temperature gradient, hence enhancing the dynamics of Marangoni convection within the molten pool. The temperature at the centre of the molten pool exceeds that at the periphery, resulting in a temperature gradient that induces a surface tension gradient towards the edge of the molten pool [10]. The liquid metal is drawn to the edge of the molten pool, while gravity causes it to flow to the bottom of the pool. As a

result, circular flows are generated in the molten pool. Further details are presented in Fig.3. at a higher magnification. The line scan's chemical composition analysis indicated that Si in the as-built alloy diminished rapidly near the interface as it dissolved into the substrate [4]. Conversely, Mg in the substrate diminished at a more gradual pace towards the powder side, thus defining the elements' dilution. Smaller intermetallic phases consist of Al, Mg, Si, Mn, and a minimal quantity of Fe is believed to be present.

The interface microstructure exhibited voids and keyholes that can adversely impact the metallurgical bond between the as-built and the cold-rolled substrate. The interfacial porosities are primarily due to aggressive thermal gradients leading to rapid solidification and gas entrapment, as well as poor melt pool wetting, causing lack of fusion defects. These phenomena can be suppressed by the Hot Isostatic Pressing (HIP) process [11], and a deep understanding of defects such as pores and cracks can be studied through X-ray Computed Tomography (XCT) [13,14]. Another way to avoid hot cracks is to preheat the substrate. This will diminish the thermal gradients, which in turn reduces thermal-induced stresses and undercooling [14-16].

The development of the metallurgical bond between the molten Al alloy powder and the substrate is heavily influenced by the interaction between the laser power beam and these two materials. As the laser beam melts the Al alloy powder and a portion of the substrate, an interface bonded zone is created. Consequently, the alloying elements from both sides amalgamated, resulting in the solidification of a layer composed of mixed alloying elements.

3.2 XRD characterisation

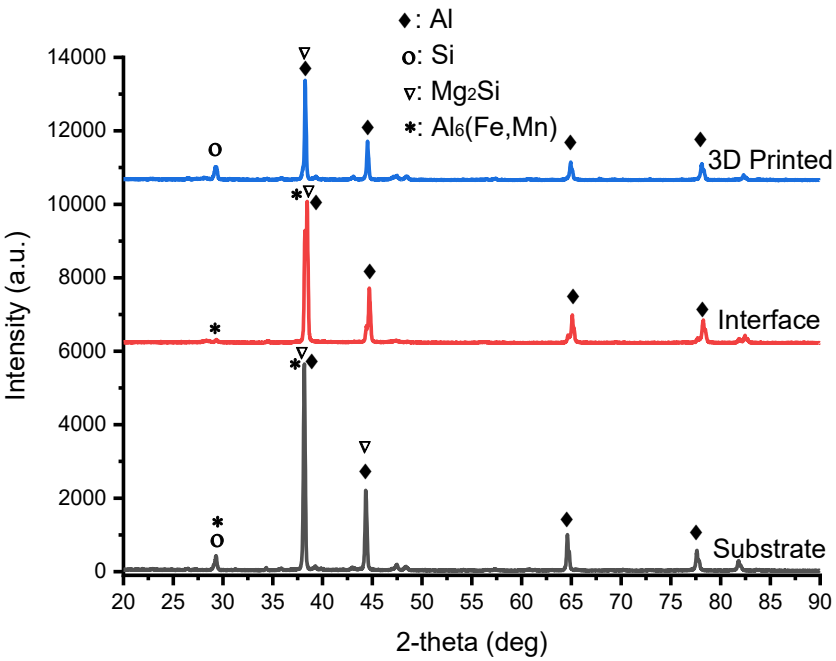

Fig. 4. XRD diffractograms recorded in the hybrid manufacturing sample.

Fig.4. displays the XRD spectral patterns of the HAM samples in both zones. A decrease in peak intensity from the substrate, interface bonded zone and the 3D printed, indicating the texture development due to respective thermal histories [16]. The cooling rate is a critical

parameter in HAM of Al-Si-Mg alloys, affecting phase distribution, segregation behaviour, and mechanical properties. Liu et al. (2018) [17] reported that the discrepancy in cooling rate of the melt pool resulted in a gradient microstructure and elemental segregation in SLM. The cooling rate at the upper surface of the melt pool attained around 1.44 × 10^6 K/s, significantly higher than that at the bottom, which is ≤ 1 × 10^3 K/s. The disparity in the cooling rate of the melt pool is the primary factor contributing to the formation of a gradient microstructure regarding the distribution of Si particles, dendritic size, sub-grains, and sub-boundaries. The XRD patterns revealed that the solidification structures in the 3D printed specimen consisted of α-Al, Si and Mg_2Si.

The spectra comparison revealed that the interface is characterised by a broader overlapping peak than that of the 3D printed and substrate around 2-theta, ranging from 38 to 38.8°, as a sign of a metastable phase denoting the dissolution of Mg_2Si and Al_6(Fe, Mg) in the α-Al matrix. The presence of metaphases like Mg_2Si, Al_6(Fe,Mn) suggested mutual diffusion of Al, Si, Mg, Mn and Fe, which can contribute to the overall strengthening of the alloy through solid solution strengthening and precipitation hardening mechanisms. The interfacial microstructure is not only influenced by alloying elements like Si, Mg, Mn and Fe, but more importantly by the cooling rate [17]. The nucleation of IMCs (intermetallic compounds) is significantly influenced by the cooling rate, with delays in nucleation occurring as the cooling rate increases. It has been reported that a higher cooling rate results in a reduction of IMCs [18].

3.3 Microhardness testing

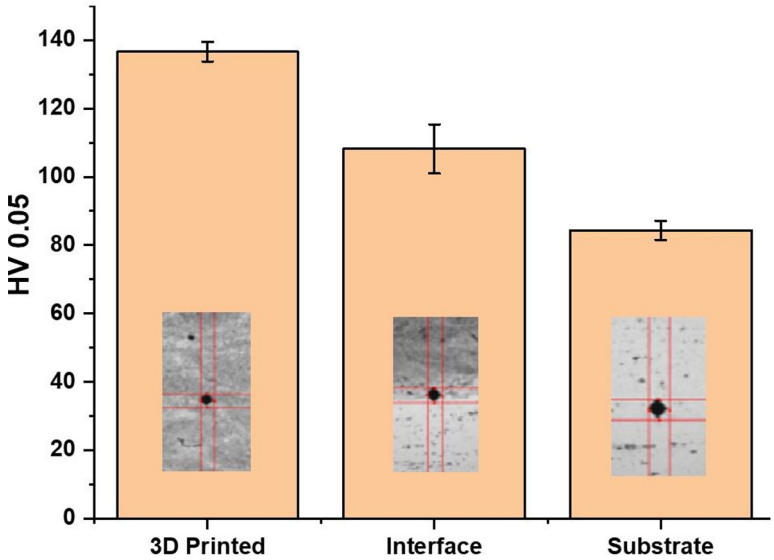

Fig. 5. Microhardness evaluation of the hybrid manufacturing sample.

The average hardness evaluation across the interface bonded zone of the hybrid specimen was determined, as illustrated in Fig. 5. The hardness of the substrate alloy was significantly inferior to that of the 3D printed, measuring 84.4 ± 2.8 HV 0.05 compared to 136.6 ± 2.9 HV 0.05, respectively. An intermediate hardness value of 108.2 ± 7.2 HV 0.05 was recorded at the interface bonded zone. The SLM-printed $AlSi_{10}Mg$ microstructure with fine grains, presence of Mg_2Si and sub-cell structures are the primary factors contributing to its exceptionally elevated hardness [19]. The high hardness value of the initially deposited layer

was ascribed to solid solution strengthening and grain refining, resulting from the dilution effect and rapid cooling rate, respectively [21,22]

4 Conclusion

The HAM process, which combines SLM with conventional SM, is a viable method for producing simple and complex engineering components on large-scale parts made of aluminium alloys. The study characterises and evaluates different phenomena and mechanisms at the interface bonding zone between the 3D printed $AlSi_{10}Mg$ and the cold-rolled AA 5083 substrate, resulting in a robust metallurgical bond. The microstructure analysis reveals a bimodal structure with equiaxed and columnar grains located near the interface in the 3D printed zone. The interface bonded zone presented a sound microstructure where dilution and diffusion of major elements occurred. The presence of metastable phases contributing to the overall microhardness of the interface-bonded zone was characterised by XRD. Microhardness measurements reveal a pronounced hardness increase at the interface bonded zone, as compared to the substrate value, suggesting diffusion and dilution of alloying elements. The findings of this study provide valuable insights into the microstructural changes and phase evolution at the interface of the HAM process, which can be used to optimise the manufacturing process and improve the material properties.

References

1. J. W. Koo, J. S. Ho, J. An, Y. Zhang, C. K. Chua, T. H. Chong, A review on spacers and membranes: Conventional or hybrid additive manufacturing?*Water Res.* **188** (2021).https://doi.org/10.1016/j.watres.2020.116497
2. D. Strong, M. Kay, B. Conner, T. Wakefield, G. Manogharan, Hybrid manufacturing – integrating traditional manufacturers with additive manufacturing (AM) supply chain. *Addit. Manuf.* **21**, 159–173 (2018).https://doi.org/10.1016/j.addma.2018.03.010
3. D. Strong, I. Sirichakwal, G. P. Manogharan, T. Wakefield, Current state and potential of additive - Hybrid manufacturing for metal parts. *Rapid Prototyp. J.* **23**, 577–588 (2017).https://doi.org/10.1108/RPJ-04-2016-0065
4. Y. L. Chan, O. Diegel, X. Xu, Evaluation of bonding integrity of hybrid-built AlSi10Mg-aluminium alloys parts using the powder bed fusion process. *Mater. Today Proc.* **46**, 1277–1282 (2021). https://doi.org/10.1016/j.matpr.2021.02.126
5. E. C. Silva, J. A. Candiango, S. J. Rodrigues, Á. M. Sampaio, J. Pontes, Hybrid Manufacturing of Aluminium Parts Combining Additive and Conventional Technologies — Mechanical and Thermal Properties. *Manuf. Mater. Process.* **6** (2022). https://doi.org/10.3390/jmmp6020040
6. A. Hadadzadeh, B. S. Amirkhiz, S. Shakerin, J. Kelly, J. Li, M. Mohammadi, Microstructural investigation and mechanical behavior of a two-material component fabricated through selective laser melting of AlSi10Mg on an Al-Cu-Ni-Fe-Mg cast alloy substrate*Addit. Manuf.* **31** (2020). https://doi:10.1016/j.addma.2019.100937.
7. A. Basak, S. Das, Epitaxy and Microstructure Evolution in Metal Additive Manufacturing. *Annu. Rev. Mater. Res.* **46**, 125–149 (2016).https://doi.org/10.1146/annurev-matsci-070115-031728
8. A. Hadadzadeh, B. Shalchi Amirkhiz, A. Odeshi, J. Li, M. Mohammadi, Role of hierarchical microstructure of additively manufactured AlSi10Mg on dynamic loading behavior. *Addit. Manuf.* **28**, 1–13 (2019).https://doi.org/10.1016/j.addma.2019.04.012

9. K. Arafune, A. Hirata, Thermal and solutal marangoni convection in In-Ga-Sb system. *J. Cryst. Growth* **197**, 811–817 (1999).https://doi.org/10.1016/S0022-0248(98)01071-9
10. Z. Zhang, H. Zhou, L. Ren, X. Tong, H. Shan, X. Li, Surface morphology of laser tracks used for forming the non-smooth biomimetic unit of 3Cr2W8V steel under different processing parameters. *Appl. Surf. Sci.* **254**, 2548–2555 (2008).https://doi.org/10.1016/j.apsusc.2007.09.102
11. L. Sun, Y. Yang, S. Li, W. Chen, Y. Wang, P. Yan, Y. Zhu, W. Wu, B. Hu, Influencing mechanisms of hot isostatic pressing on surface properties of additively manufactured AlSi10Mg alloy. *J. Mater. Process. Technol.* **329**, 118426 (2024).https://doi.org/10.1016/j.jmatprotec.2024.118426
12. P. D. Nezhadfar, S. Thompson, A. Saharan, N. Phan, N. Shamsaei, Structural integrity of additively manufactured aluminum alloys: Effects of build orientation on microstructure, porosity, and fatigue behavior. *Addit. Manuf.* **47**, 102292 (2021).https://doi.org/10.1016/j.addma.2021.102292.
13. Y. Mao, H. Chen, J. Xiong, Research progress in laser additive manufacturing of aluminum alloys: Microstructure, defect, and properties. *J. Mater. Res. Technol.* **30**, 695–716 (2024).https://doi.org/10.1016/j.jmrt.2024.03.099
14. S. Z. Uddin, L. E. Murr, C. A. Terrazas, P. Morton, D. A. Roberson, R. B. Wicker, Processing and characterization of crack-free aluminum 6061 using high-temperature heating in laser powder bed fusion additive manufacturing. *Addit. Manuf.* **22**, 405–415 (2018).https://doi.org/10.1016/j.addma.2018.05.047
15. Y. Shi, K. Yang, S. K. Kairy, F. Palm, X. Wu, P. A. Rometsch, Effect of platform temperature on the porosity, microstructure and mechanical properties of an Al–Mg–Sc–Zr alloy fabricated by selective laser melting. *Mater. Sci. Eng. A* **732**, 41–52 (2018).https://doi.org/10.1016/j.msea.2018.06.049
16. H. Gu, L. Bhatta, H. Gao, Z. Li, C. Kong, H. Yu, Effect of cryorolling on the microstructure and high-temperature mechanical properties of AA5083 sheets*Mater. Sci. Eng. A* **843** (2022). https://doi:10.1016/j.msea.2022.143141.
17. Y. J. Liu, Z. Liu, Y. Jiang, G. W. Wang, Y. Yang, L. C. Zhang, Gradient in microstructure and mechanical property of selective laser melted AlSi10Mg. *J. Alloys Compd.* , 1414e1421 (2018).https://doi.org/10.1016/j.jallcom.2017.11.020
18. Y. Liu, M. Liu, L. Luo, J. Wang, C. Liu, The solidification behavior of AA2618 aluminum alloy and the influence of cooling rate. *Materials (Basel).* **7**, 7875–7890 (2014).https://doi: 10.3390/ma7127875
19. P. Snopiński, K. Matus, F. Tatiček, S. Rusz, Overcoming the strength-ductility trade-off in additively manufactured AlSi10Mg alloy by ECAP processing. *J. Alloys Compd.* **918** (2022). https://doi:10.1016/j.jallcom.2022.165817.
20. S. Shakerin, A. Hadadzadeh, B. S. Amirkhiz, S. Shamsdini, J. Li, M. Mohammadi, Additive manufacturing of maraging steel-H13 bimetals using laser powder bed fusion technique. *Addit. Manuf.* **29**, 100797 (2019).https://doi.org/10.1016/j.addma.2019.100797
21. A. Hadadzadeh, B. S. Amirkhiz, S. Shakerin, J. Kelly, J. Li, M. Mohammadi, Microstructural investigation and mechanical behavior of a two-material component fabricated through selective laser melting of AlSi10Mg on an Al-Cu-Ni-Fe-Mg cast alloy substrate. *Addit. Manuf.* **31**, 100937 (2020). https://doi.org/10.1016/j.addma.2019.100937